Journal of Applied Polymer Science

Disappearance of the filler—An interesting interfacial evolution during the photooxidative aging of polypropylene composites

Jiaohong Zhao, Xuan Liu, Rui Yang, Jian Yu
Key Laboratory of Advanced Materials, Ministry of Education, Department of Chemical Engineering, Tsinghua University, Beijing 100084, People's Republic of China
Correspondence to: R. Yang (E-mail: yangr@mail.tsinghua.edu.cn)

ABSTRACT: The interface between the matrix and filler in polyolefin composites plays an important role in their photooxidative aging processes. An interesting phenomenon, the gradual disappearance of filler particles was observed during the early natural aging of polypropylene (PP)/$CaCO_3$ composites. Similar phenomena were also observed in a PP/SiO_2 composite and PP/poly(methyl methacrylate) blend. The morphological observation and tensile and chemical analyses indicated that the photooxidized groups of the PP chain interacted strongly with the filler particles; this increased the tensile strength during the early aging stage. The PP matrix was entangled in the filler particles. Therefore, the filler particles were embedded in the matrix, and the fracture occurred in the PP matrix instead of at the interface between them. On the basis of these results, a "disappearing" filler mechanism for the PP composites was proposed. This work provides a possible way for improving the mechanical properties of PP composites with appropriate aging. © 2015 Wiley Periodicals, Inc. J. Appl. Polym. Sci. **2015**, *132*, 42546.

KEYWORDS: aging; degradation; polyolefins

Received 22 March 2015; accepted 26 May 2015
DOI: 10.1002/app.42546

INTRODUCTION

Polyolefin/filler composites have been widely used in industry because of their good comprehensive performance, in particular, their balanced toughness and strength. Fillers are used to improve the mechanical properties, barrier performance, heat resistance, and so on of the polyolefin polymer. However, the filler can also interfere with the photooxidative aging of the matrix because of its metal ions, photo or heat sensitivity, nucleation effect, and filler particle size and content.[1–7] Most of these interferences occur at the matrix/filler interface or on the surface of the filler particles. However, only little attention has been paid to the effects of the filler surface on the aging of the matrix.[2,8–10] Yang *et al.*[2] reported that Fe^{2+} ions initiated the free-radical reaction and catalyzed the decomposition of hydroperoxide to form carbonyl groups; this led to chain scission. The active sites of montmorillonite, brought by the complicated crystal structure and ammonium salts, can accept electrons from matrix, which can accelerate the aging of polyolefin.[8] Dintcheva *et al.*[11] found that the formation of carboxylic salts at the interface between the matrix and filler in the PP/$CaCO_3$ (PP/$CaCO_3$) composite could have been one of the reasons for the higher aging rate of the nanocomposite compared to that of the microcomposite. Yang *et al.*[10] demonstrated that different surface treatments of $CaCO_3$ particles resulted in different aging degrees of the PP/$CaCO_3$ composite. It is believed that the total surface area and surface groups affect the aging process of a composite.

There have been a few reports on interfacial changes in polymer blends during aging.[12–16] Kaczmarek *et al.*[12,13] reported that the morphology of the polymer near the phase interfaces in both poly(methyl methacrylate) (PMMA)/polystyrene and polyvinyl acetate (PVAc)/polystyrene blends significantly changed during UV-irradiated aging. In addition, a small amount of copolymer formed to act as a compatibilizer, which enhanced the miscibility. Fernandes *et al.*[14] reported that the increasing the high impact polystyrene (HIPS) concentration in PP/HIPS composites affected the interface between the polymers and thus resulted in better photostability in the composite. Dintcheva *et al.*[15] found that the addition of organo-montmorillonite (OMMT) changed the morphology of a polyethylene (PE)/polyamide (PA) blend. The poor interfacial adhesion and low specific interfacial area hindered the propagation of the degradation products of the surfactant in organoclay and also inhibited the diffusion of PA radicals into the PE phase. Therias *et al.*[16] found that the oxygenated radicals in aged PA initiated the oxidation of PE chains and accelerated the aging of PE.

To the best of our knowledge, there has been no report on the interfacial evolution during the aging of polymer composites or about the effects of interfacial changes during aging on the

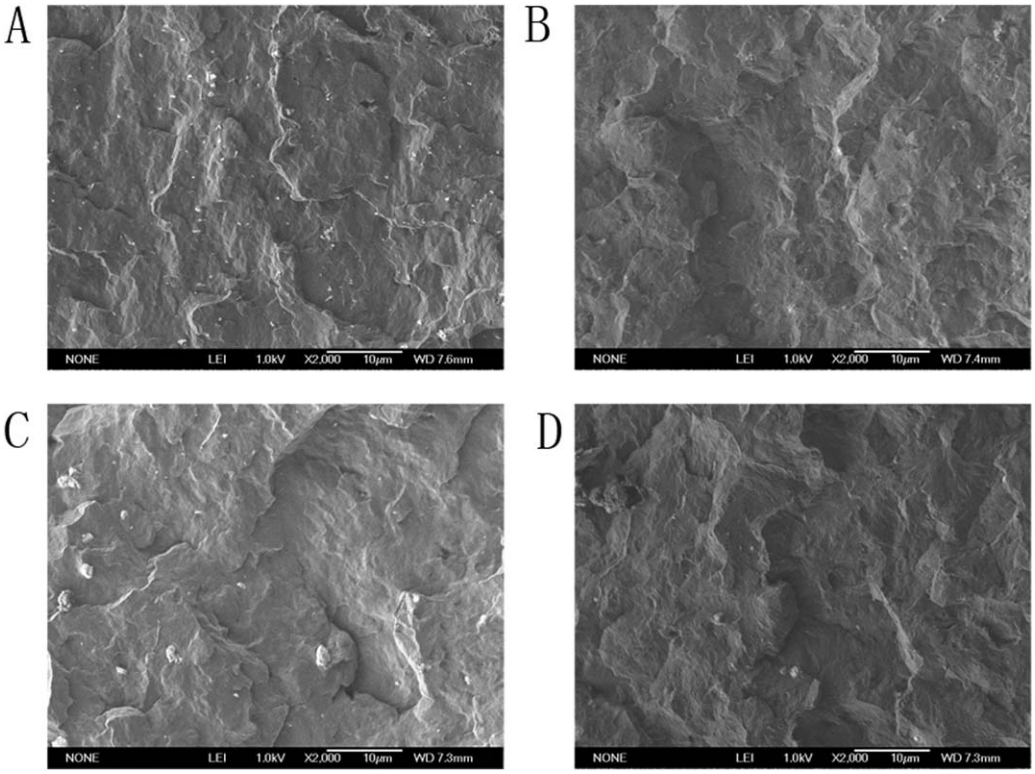

Figure 1. Cross-sectional SEM images of the (A,B) PP/nano-$CaCO_3$ and (C,D) PP/micro-$CaCO_3$ composites (A,C) before and (B,D) after 120 days of aging.

aging of composites. In this study, the disappearance of filler particles was found in the cross section of the PP/$CaCO_3$ composite after photooxidative aging. The interfacial cohesion was enhanced during the aging process under UV irradiation; this further increased the tensile strength. The mechanism was discussed. This phenomenon also occurred in other PP composites and blends, such as a PP/SiO_2 composite and PP/PMMA blend. A mechanism for the disappearance of the fillers was proposed. The results indicate that appropriate aging may be useful in the improvement of the mechanical properties of PP composites.

EXPERIMENTAL

Materials

Isotactic PP (S1003, melt flow index = 3.2 g/10 min) was from Yanshan Petrochemical Co., Ltd. (Beijing, China). Nano-$CaCO_3$ (70 nm) was provided by East China University of Science and Technology. Micro-$CaCO_3$ (1250 mesh) was obtained from Guoli Superfine Fillers Co., Ltd. (Beijing, China). Nano-SiO_2 (70 nm) and micro-SiO_2 (1 μm) were prepared in our laboratory. PMMA (molecular weight = 1.1×10^5 g/mol, Mitsubishi Electric Co.) was used as received.

Sample Preparation and Aging

PP/$CaCO_3$ and PP/SiO_2 composites and PP/PMMA blends were prepared by the melt blending of PP with $CaCO_3$, SiO_2 and PMMA, respectively, in a Haake PolyDrive mixer (Thermo Electron Co.) at 60 rpm at 190°C. The composites and blends were hot-pressed to form 375-μm films and 2-mm plates, respectively. The accelerated aging was conducted by the irradiation of the samples under 180 W/m^2 UV light at 40°C in a Xenon artificial weathering system (Chongqing HanZhan Instrument Co., Ltd.) for up to 12 days. Natural aging was performed through

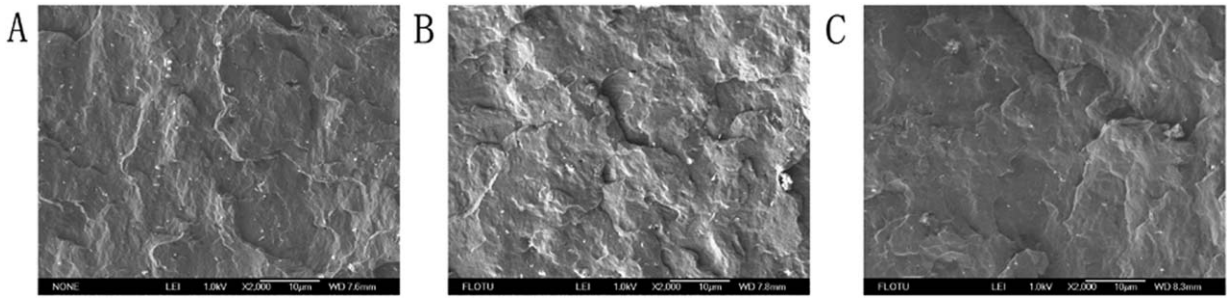

Figure 2. Cross-sectional SEM images of the PP/nano-$CaCO_3$ composites aged for (A) 0, (B) 19, and (C) 25 days.

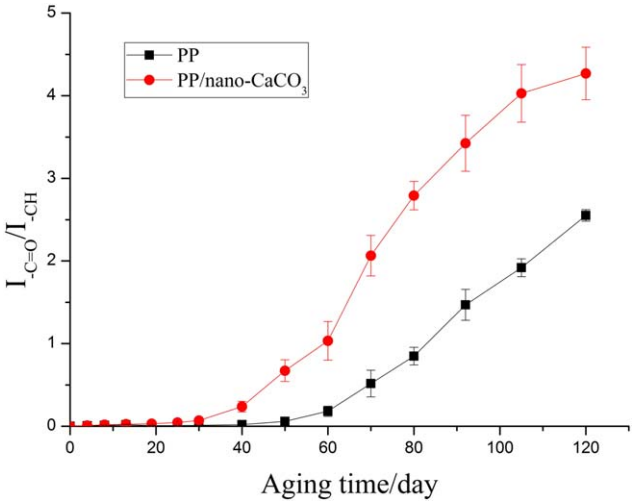

Figure 3. Carbonyl index changes of the PP and PP/nano-$CaCO_3$ composite with increasing aging time.[10] [Color figure can be viewed in the online issue, which is available at wileyonlinelibrary.com.]

exposure of the samples to the natural outdoor environment for up to 120 days.

Characterization

The Fourier transform infrared (FTIR) spectra were obtained on a Thermo-Nicolet 6700 FTIR spectrometer. We obtained the transmission spectra of the film samples by averaging 32 scans at a resolution of 4 cm^{-1} in the range 400–4000 cm^{-1}. The sample plates were cut into 20 μm thick sectional slices with a microtome (YD-1508R, Zhejiang Jinhua Yidi Medical Equipment Factory, Hangzhou, China) and analyzed along the depth on a Nicolet Continuum FTIR microscope with an aperture of 100 × 100 μm^2. The peak at 2720 cm^{-1} was used as a reference and was associated with the combination of CH bending and CH_3 stretching.[17] The ratio of the carbonyl absorbance to the reference is defined as the *carbonyl index* ($I_{-C=O}/I_{-CH}$).

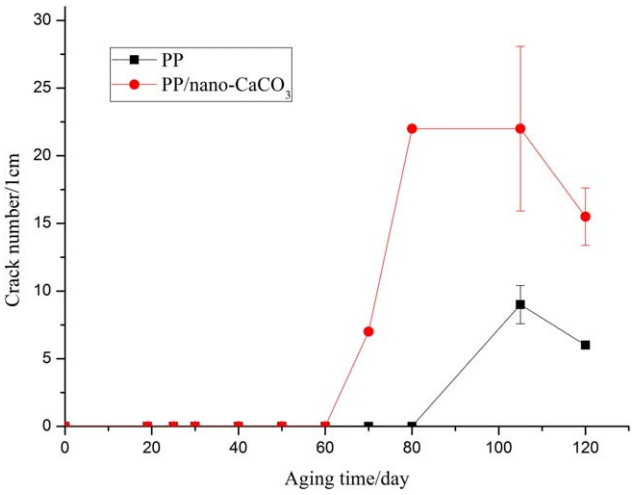

Figure 4. Crack generation of the PP and PP/nano-$CaCO_3$ composites during natural aging. [Color figure can be viewed in the online issue, which is available at wileyonlinelibrary.com.]

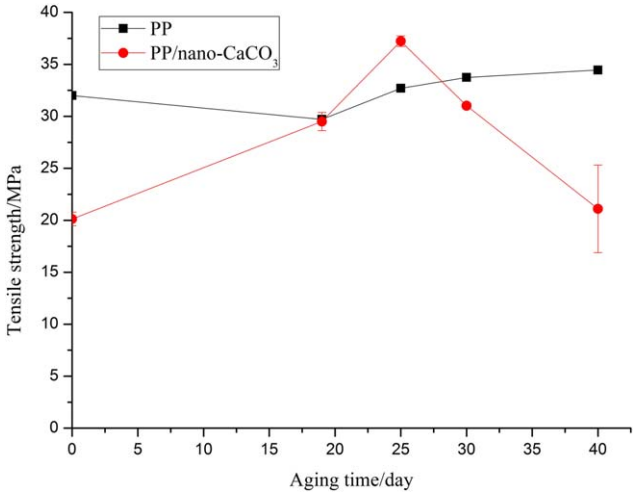

Figure 5. Tensile strength changes of the PP and PP/nano-$CaCO_3$ composite with increasing aging time. [Color figure can be viewed in the online issue, which is available at wileyonlinelibrary.com.]

Differential scanning calorimetry measurement was carried out on a Q100 calorimeter (TA Instruments) to study the melting and crystallization behaviors of the composites. The samples were heated from room temperature to 220°C at 10°C/mina; heating was halted at 220°C for 3 min, and then, the sample was cooled to room temperature at 10°C/min. The transition temperature and enthalpy were recorded, and the crystallinity was calculated accordingly.[18,19]

The volatile photooxidation degradation products of the samples were analyzed with a pyrolysis gas chromatograph/mass spectrometer (PGC–MS; Shimadzu GCMS-QP5050A) equipped with a PYR 4A pyrolyzer. The chain-scission-induced small molecules from the macromolecules were determined by the flash evaporation technique. About 1 mg of sample was flash-heated at 300°C for 30 s. The small molecules were separated in a fused silica capillary column (DB-5 25 μm × 0.25 mm *i.d.*) with He as the carrier gas and detected with an MS detector.

The cryogenically fractured cross sections were imaged on a JSM-7401 field emission scanning electron microscope at an accelerating voltage of 1 kV.

For the tensile strength measurements, the samples were tested in a TCS-2000 tensile tester (Gotech) operating at an extension speed of 2 mm/min at 25°C with rectangular-shaped samples.

RESULTS AND DISCUSSION

Filler Disappearance in the PP/$CaCO_3$ Composites during Aging

The PP/nano-$CaCO_3$ and PP/micro-$CaCO_3$ composites were aged outdoors for 120 days. Their cross-sectional morphologies before and after aging were imaged, as shown in Figure 1. Both nano-$CaCO_3$ and micro-$CaCO_3$ particles were observed clearly in the composites without aging and showed clear boundaries with the PP matrix; this indicated poor interfacial cohesion between the filler and the matrix [Figure 1(A,C)]. Figure 1(B,D) shows the morphologies of the composites aged naturally for

Table I. Changes in the Melting Temperature and Crystallinity of the PP and PP/nano-$CaCO_3$ Composite during Natural Aging

	Melting temperature (°C)		Crystallinity	
Time (day)	PP	PP/nano-$CaCO_3$	PP (%)	PP/nano-$CaCO_3$ (%)
0	164.6	164.5	41.8	44.5
19	165.0	165.0	43.8	41.9
25	164.3	165.0	42.6	42.1
30	165.1	164.8	39.7	42.9
40	161.2	164.4	44.1	41.5

120 days. Surprisingly, the $CaCO_3$ particles could not be observed clearly after aging. They disappeared!

To determine how the filler particles disappeared in the composite, the morphological evolution of the PP composites during the early aging stage was monitored. Because the PP/nano-$CaCO_3$ and PP/micro-$CaCO_3$ composites showed similar morphologies and aging mechanisms,[10] only the PP/nano-$CaCO_3$ composite is discussed in the following text. As shown in Figure 2, the morphology of the composite was significantly changed after the composite was aged for 25 days. The $CaCO_3$ particles appeared to be embedded in the PP matrix. The chemical evolution of the composites during aging was also

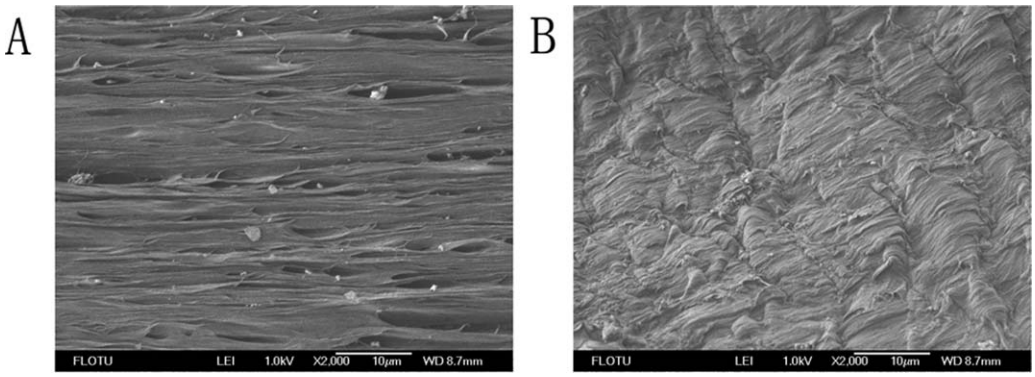

Figure 6. SEM images of the tensile cross section of the PP/$CaCO_3$ composites (paralleled to stretching direction) (A) before and (B) after aging for 19 days.

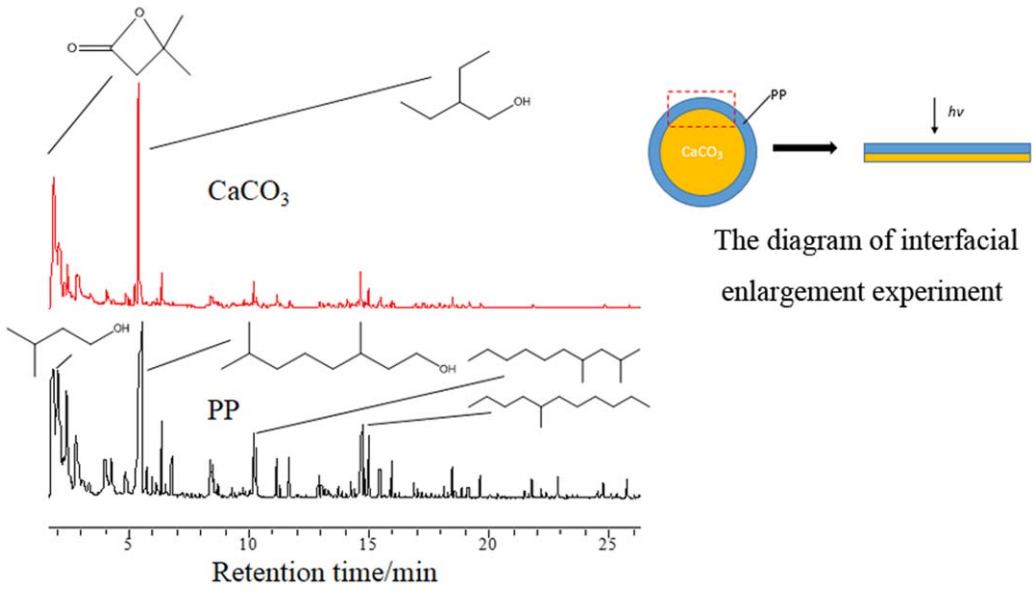

Figure 7. PGC–MS chromatograms of the PP sheet and $CaCO_3$ sampled from the contact surface after photooxidative aging (pyrolysis temperature = 600°C). $h\nu$ = energy of ultraviolet light; h = Planck constant; ν = frequency. [Color figure can be viewed in the online issue, which is available at wileyonlinelibrary.com.]

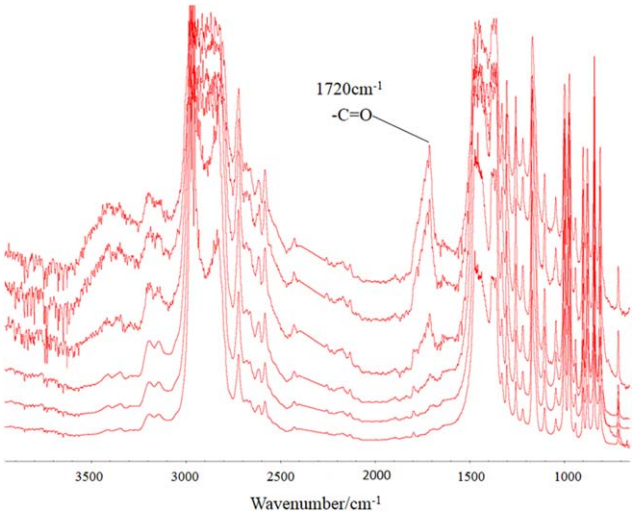

Figure 8. FTIR spectra of the aged PP/nano-$CaCO_3$ composites along the depth from the surface to the interior at 45, 90, 130, 185, 310, and 490 μm (from top to bottom in order). [Color figure can be viewed in the online issue, which is available at wileyonlinelibrary.com.]

determined with FTIR spectroscopy. The results show that the carbonyl index was not significantly increased before the composite was aged for 30 days (Figure 3). Nearly no crack was first observed on the film surface of the composite aged for 50 days (Figure 4).

The previous results show that photooxidation of PP initially occurred at the interface. The carbonyl index remained unchanged at the early aging stage because of the low concentration of the oxidative products at the interface. During the aging process, the oxidative groups of the aged PP chains strongly interacted with the $CaCO_3$ particles and entangled with the filler particles. Thus, the composite was broken in the PP matrix instead of on the interface when it was fractured in liquid nitrogen. Therefore, the $CaCO_3$ particles seemed to

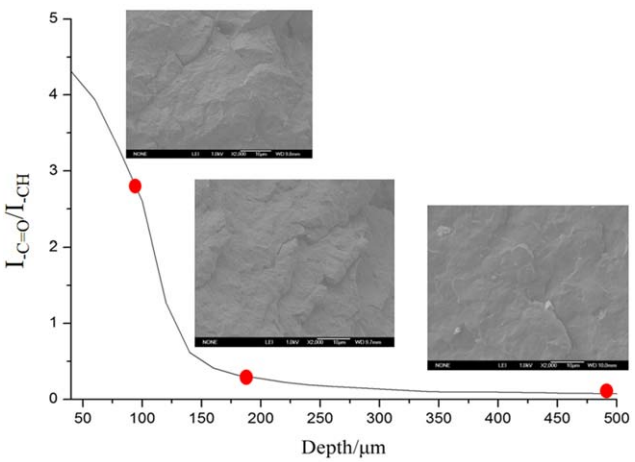

Figure 9. Carbonyl index profile of the aged bulk PP/nano-$CaCO_3$ composites along the depth from the surface to the interior and the corresponding cross-sectional SEM images. [Color figure can be viewed in the online issue, which is available at wileyonlinelibrary.com.]

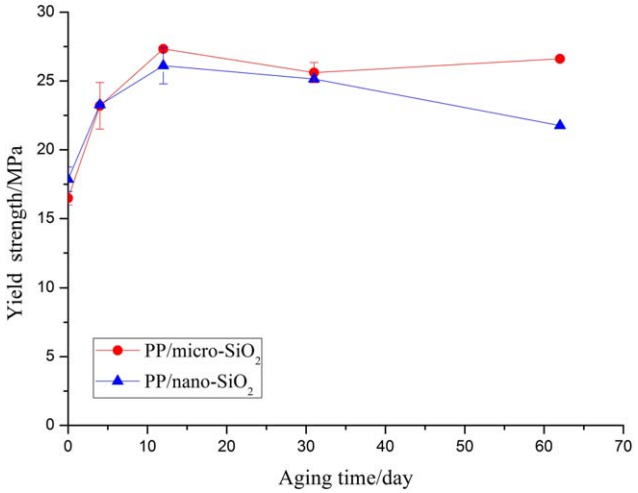

Figure 10. Tensile strength changes of the PP/nano-SiO_2 and PP/micro-SiO_2 composites with increasing aging time. [Color figure can be viewed in the online issue, which is available at wileyonlinelibrary.com.]

disappear in the composites when they were observed on cross section.

To verify our hypothesis, the tensile strengths of the PP and PP/nano-$CaCO_3$ composite were tested (Figure 5). The tensile strength of PP alone remained nearly unchanged during the first 40 days of exposure. In contrast, the tensile strength of the PP/nano-$CaCO_3$ composite increased during the first 25 days of aging and decreased thereafter. It is known that crystallization can enhance the mechanical properties of materials. However, it remains unclear whether the crystallization caused by segmental movement at the early stage of aging contributed to the increase in the tensile strength in this case. Table I shows the melting temperature and crystallinity values of the PP and PP/nano-$CaCO_3$ composite during natural aging. No obvious changes were observed for both the melting temperature and crystallinity of the PP/nano-$CaCO_3$ composite in the first 30 days of aging; this indicated that crystallization was not the dominant factor responsible for the increased tensile strength of the aged PP/nano-$CaCO_3$ composite. Figure 6 shows the tensile cross-sectional scanning electron microscopy (SEM) images of the PP/$CaCO_3$ composite before and after aging for 19 days. The $CaCO_3$ particles could be easily identified in the cavities of the nonaged PP/$CaCO_3$ composite under stretching; this indicated that the cavities were generated because of the poor interfacial cohesion between the $CaCO_3$ particles and PP matrix. No obvious boundary between the PP and $CaCO_3$ particles was observed on the aged tensile cross section; this indicated that the breakage occurred in the matrix instead of at the interface. This result further provided evidence for stronger interactions between the $CaCO_3$ particles and PP matrix. Thus, the interfacial strength improved, and the interface between $CaCO_3$ and PP was not easily broken during stretching by tensile testing.

The increased interfacial interaction was also demonstrated by the PGC–MS analysis of the $CaCO_3$ particles directly in contact with PP in a model experiment.[10] A $CaCO_3$ suspension was dispersed on a PP sheet and irradiated with UV light from the PP

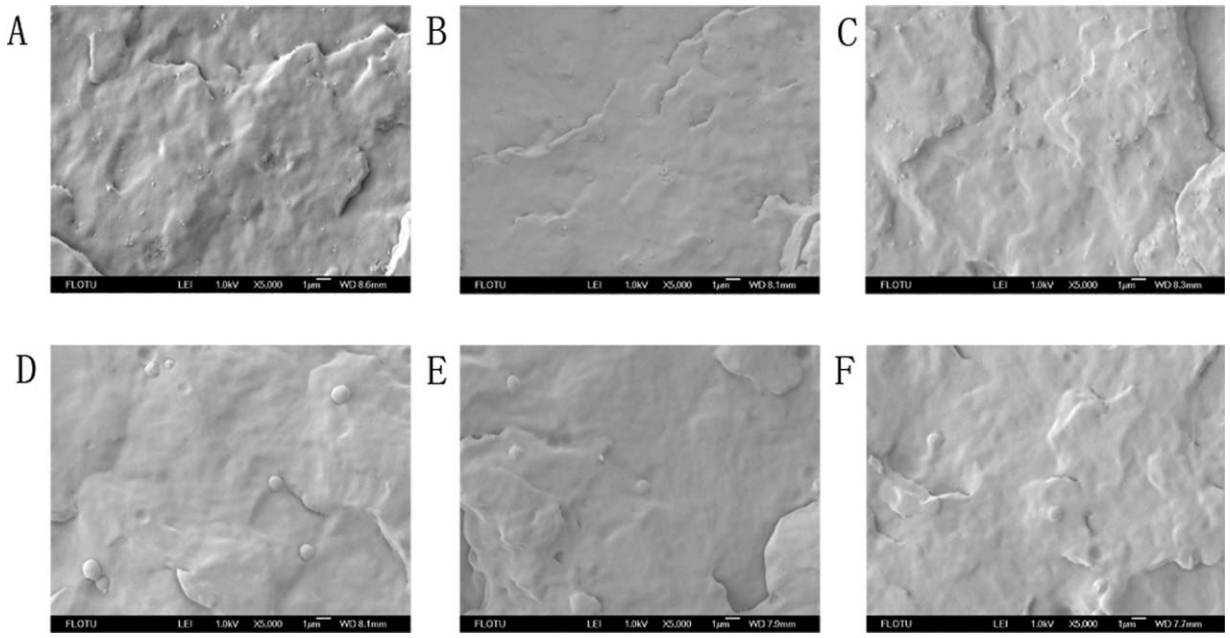

Figure 11. SEM images of the (A–C) PP/nano-SiO_2 and (D–F) PP/micro-SiO_2 composites (A,D) before aging and after aging for (B,E) 31 and (C,F) 62 days.

sheet side. The PP sheet and $CaCO_3$ particles were sampled from the contacting surface and pyrolyzed at 600°C. Their PGC–MS chromatograms are shown in Figure 7. Most peaks on the chromatogram of the aged PP could be attributed to the photooxidative degradation products of the PP chains, including alkanes, cycloesters, and branched aliphatic alcohols. Similar fragments were also found on the chromatogram of $CaCO_3$ particles; this indicated that the oxidative products of PP were attached to the surface of the $CaCO_3$ particles after the aging. Therefore, these organized $CaCO_3$ particles had improved compatibility with the matrix, and the interfacial reaction increased after aging.

To illustrate the photooxidation-induced interfacial interaction improvement further, we investigated the photooxidative aging of bulk PP/nano-$CaCO_3$ composites. The FTIR spectra of the aged bulk composite at different depths are shown in Figure 8. Its carbonyl index profile along the depth from the surface to the interior and the corresponding SEM images are shown in Figure 9. The intensity of the characteristic peaks of the oxidative products at 1720 cm^{-1} was higher near the surface and gradually decreased along the depth from the surface to the interior. No carbonyl and hydroxyl groups were observed at positions deeper than 185 μm. The oxidation profile also showed that the carbonyl index decreased with increasing depth because of the limited oxygen diffusion (Figure 9). It is worth noticing that no $CaCO_3$ particles were observed at the positions where the oxidation degree was relatively high, and the $CaCO_3$ particles gradually appeared with decreasing oxidation degree. This further demonstrated that the photooxidation of PP at the interface improved its compatibility and enhanced the interfacial strength between the two phases. The breakage occurred in the PP matrix instead of on the interface when the composite was cryogenically fractured. Thus, no $CaCO_3$ particles were observed at positions near the surface where the oxidation degree was high. In contrast, the $CaCO_3$ particles could be identified in the positions where the oxidation degree was low and the interfacial strength was weak. Breakage occurred on the interface between the two phases.

In full, the $CaCO_3$ particles disappeared in the cross-sectional SEM images during natural aging. This phenomenon could be attributed to the strong interactions between the oxidative groups of the aged PP and $CaCO_3$ particles. The aged PP

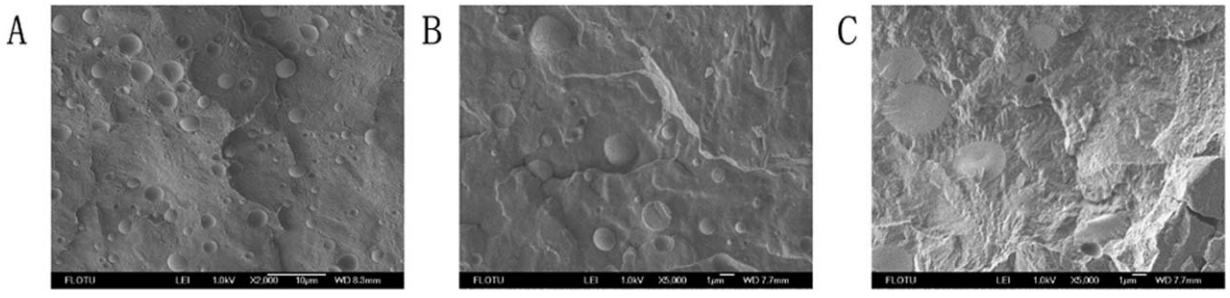

Figure 12. Cross-sectional SEM images of the PP/PMMA (90/10) blend aged for (A) 0, (B) 4, and (C) 12 days under UV irradiation.[1]

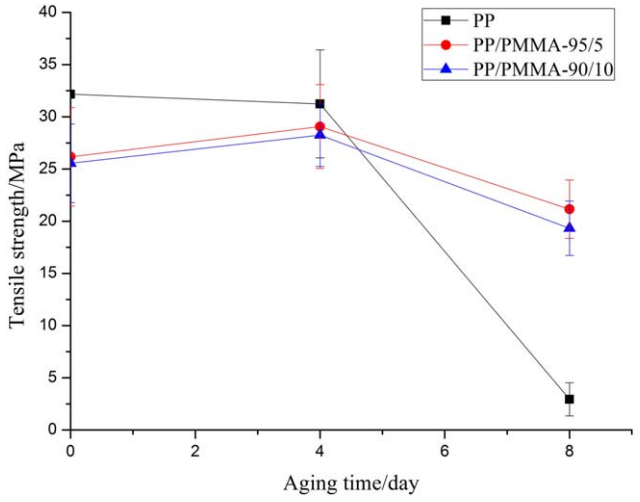

Figure 13. Tensile strength changes of the PP and PP/PMMA blends with increasing aging time. [Color figure can be viewed in the online issue, which is available at wileyonlinelibrary.com.]

molecular chains were entangled in the $CaCO_3$ particles; this enhanced the interfacial strength. Therefore, the cryogenic breakage occurred in the aged PP matrix instead of on the surface between the two phases, and the $CaCO_3$ particles disappeared in the composite. In addition, the improved interfacial interaction also led to increased tensile strength at early aging when most of the matrix was not aged, and no occurrence of oxidation was observed in the FTIR spectra. This further confirmed that aging was prone to begin from the interface between the matrix and filler in the composites.[20]

Filler Disappearance in Other Composites

SiO_2 is also widely used to reinforce polyolefin polymers. Its abundant surface hydroxyl groups can probably interact with the oxidative groups of the aged PP. Therefore, the filler disappearance phenomena was also observed in the PP/SiO_2 composite. Figure 10 shows the tensile strength changes of the PP/SiO_2 composites with increasing aging time. The tensile strengths of both the PP/nano-SiO_2 and PP/micro-SiO_2 composites increased during the early aging stage. The SiO_2 particles gradually disappeared during the aging process (Figure 11). Many fewer bare SiO_2 particles were observed after the composite was aged for 31 days. The result indicates the better interfacial

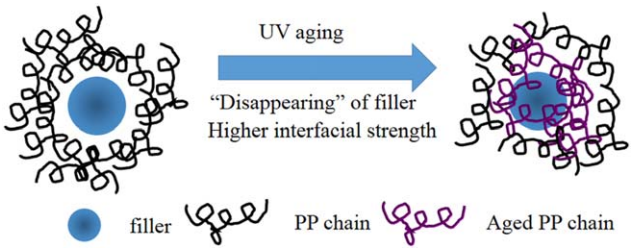

Scheme 1. Morphological evolution during the early aging of the PP composites. [Color figure can be viewed in the online issue, which is available at wileyonlinelibrary.com.]

compatibility of the PP composites induced by photooxidative aging, and the increased tensile strength was closely related to the improvement of the interfacial compatibility. A similar phenomenon appeared in Rabello *et al.*'s[21] work, in which the tensile strength of talc-filled composite increased slightly during the early aging stage.

Disappearance of the Dispersed Phase in the PP Blend

In addition to PP composites with inorganic fillers as the dispersed phase, we also extended our study to PP blends to investigate if the photooxidation-induced interfacial reinforcement and corresponding morphological change was a universal phenomenon. In this study, the changes in the morphology and tensile strength of the PP/PMMA blend during aging were investigated. Figure 12 shows the cross-sectional SEM images of the PP/PMMA blends aged for 0, 4, and 12 days. It was clear that the dispersed PMMA particles gradually disappeared in the PP matrix during photooxidative aging.[1] Similarly, the interfacial interaction between PP and PMMA was weak, and a clear boundary was observed between them before the blend was aged. The boundary became vague after the blend was aged for 4 days. No PMMA particles were obvious after the blend was aged for 12 days. In addition, fracturing occurred in the PP matrix and PMMA particles at places other than the interface.

The tensile strength of the PP/PMMA blend was nearly unchanged (or slightly increased somehow) after the blend was aged for 4 days (Figure 13). The change in the tensile strength of the PP/PMMA blend was not as significant as that of the PP/$CaCO_3$ composite during the early aging stage. It could be explained that the PMMA particle was much bigger than the $CaCO_3$ particle. The interfacial area between PMMA and PP

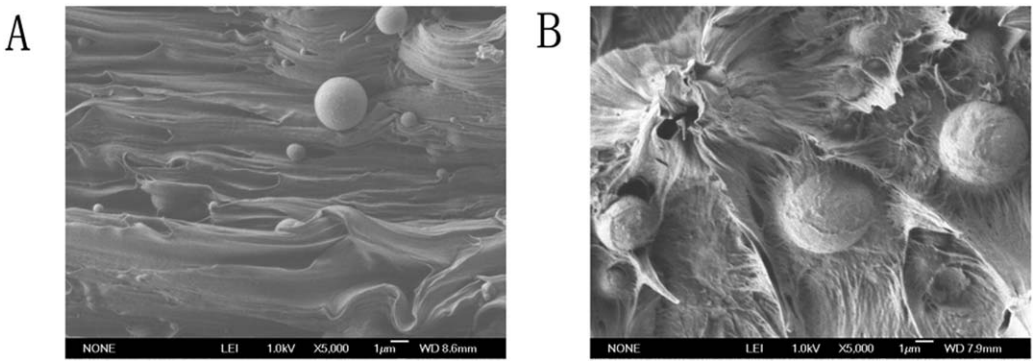

Figure 14. SEM images of the tensile cross sections of the PP/PMMA (90/10) (A) before and (B) after aging for 8 days.

was smaller, and the photooxidation-induced interfacial interaction did not change significantly.

The cross-sectional SEM images of the tensile PP/PMMA blend before and after aging are shown in Figure 14. Smooth PMMA particles were well dispersed in the blend before aging. The PMMA particles became very rough and were intensively grabbed by the PP matrix after the composite was aged for 8 days. It has been reported that chemical bonding between PP and PMMA occurs during photooxidative aging.[1] Therefore, chemical bonding can enhance the interfacial strength and increase the tensile strength during the early stage of aging.

On the basis of the previous discussion, the disappearance mechanism of the filler in the PP composites is proposed as illustrated in Scheme 1. PP molecules near the interface with filler particles were subjected to oxidation under UV irradiation and strongly interacted with the filler particles; this enhanced the interfacial cohesion. Some of PP chains were even grafted on the dispersed particles under irradiation. The tensile strength increased with the improvement of interfacial strength. Therefore, fracture occurred in the PP matrix instead of at the interface between the matrix and filler, and the filler seemed to disappear in the PP matrix from the cross-sectional morphology. This work provides a possible way to increase the interfacial interaction between PP and fillers *in situ* and thus improve the mechanical properties by controlled slight aging.

CONCLUSIONS

In this study, an interesting morphological change during the photooxidative aging of PP composites and PP blends was observed: filler particles or the dispersed phase disappeared on the cross section. The oxidized PP molecules under UV irradiation showed better compatibility with the dispersed phase. Some of them were even grafted onto the dispersed phase. The inorganic fillers or the organic blends tended to be embedded in the PP matrix because of the increased interfacial strength. Therefore, the fracture occurred in the PP matrix instead of at the interface between the PP matrix and the filler. The tensile strengths of the PP composites and blends increased in the early aging stage. This phenomenon occurred in many PP composites and blends, such as PP/$CaCO_3$ composites, PP/SiO_2 composites, and PP/PMMA blends. This is the first time interfacial changes of polyolefin composites during photooxidative aging and their effects on the properties of the composites have been revealed. Future work will be focused on whether the prerequisites for a composite or a blend can cause stronger interfacial strength and higher tensile strength in aged composites.

ACKNOWLEDGMENTS

This project was supported by Natural Science Foundation of China (NSFC) (Project 21274078).

REFERENCES

1. Zhao, J. H.; Yang, R.; Yu, J. *Polym. Degrad. Stab.* **2013**, *98*, 1981.
2. Qin, H. L.; Zhang, Z. G.; Feng, M.; Gong, F. L.; Zhang, S. M.; Yang, M. S. *J. Polym. Sci. Part B: Polym. Phys.* **2004**, *42*, 3006.
3. La Mantia, F. P.; Dintcheva, N. T.; Malatesta, V.; Pagani, F. *Polym. Degrad. Stab.* **2006**, *91*, 3208.
4. Zhao, H. X.; Li, R. K. Y. *Polymer* **2006**, *47*, 3207.
5. Allen, N. S.; Edge, M.; Ortega, A.; Sandoval, G.; Liauw, C. M.; Verran, J.; Stratton, J.; McIntyre, R. B. *Polym. Degrad. Stab.* **2004**, *85*, 927.
6. Li, J. F.; Yang, R.; Yu, H.; Liu, Y. *Polym. Degrad. Stab.* **2008**, *93*, 84.
7. Yang, R.; Liu, Y.; Yu, J.; Zhang, D. Q. *Polym. Eng. Sci.* **2008**, *48*, 2270.
8. Qin, H. L.; Zhang, S. M.; Liu, H. J.; Xie, S. B.; Yang, M. S.; Shen, D. Y. *Polymer* **2005**, *46*, 3149.
9. Morlat-Therias, S.; Mailhot, B.; Gardette, J. L.; Da Silva, C.; Haidar, B.; Vidal, A. *Polym. Degrad. Stab.* **2005**, *90*, 78.
10. Zhao, J. H.; Yang, R.; Yu, J. *Acta Polym. Sinica* **2014**, *12*, 1600.
11. Morreale, M.; Dintcheva, N. T.; La Mantia, F. P. *Polym. Int.* **2011**, *60*, 1107.
12. Kaczmarek, H. *Polymer* **1996**, *37*, 547.
13. Nowicki, M.; Kaczmarek, H.; Czajka, R.; Susła, B. *J. Vacuum Sci. Technol. A* **2000**, *18*, 2477.
14. Fernandes, L. L.; Freitas, C. A.; Demarquette, N. R.; Fechine, G. J. M. *J. Appl. Polym. Sci.* **2011**, *120*, 770.
15. Dintcheva, N. T.; Filippone, G.; La Mantia, F. P.; Acierno, D. *Polym. Degrad. Stab.* **2010**, *95*, 527.
16. Therias, S.; Dintcheva, N. T.; Gardette, J. L.; La Mantia, F. P. *Polym. Degrad. Stab.* **2010**, *95*, 522.
17. Rabello, M. S.; White, J. R. *Polym. Degrad. Stab.* **1997**, *56*, 55.
18. Wan, W. T.; Yu, D. M.; Xie, Y. C.; Guo, X. S.; Zhou, W. D.; Cao, J. P. *J. Appl. Polym. Sci.* **2006**, *102*, 3480.
19. Turi, E. A. Thermal Characterization of Polymeric Materials; Academic: New York, **1981**.
20. Knight, J. B.; Calvert, P. D.; Billingham, N. C. *Polymer* **1985**, *26*, 1713.
21. Rabello, M. S.; White, J. R. *Polym. Compos.* **1996**, *17*, 691.